Journal of Power Sources 196 (2011) 7277–7289

Contents lists available at ScienceDirect

Journal of Power Sources

journal homepage: www.elsevier.com/locate/jpowsour

Development of an integrated gasifier–solid oxide fuel cell test system: A detailed system study

Ming Liu [a,*], P.V. Aravind [a], T. Woudstra [a], V.R.M. Cobas [b], A.H.M. Verkooijen [a]

[a] Delft University of Technology, Energy Technology Section, Leeghwaterstraat 44, 2628 CA Delft, The Netherlands
[b] Federal University of Itajuba, Department of Mechanical Engineering, Pinheirinhos 37500-903, MG, Brazil

ARTICLE INFO

Article history:
Received 16 December 2010
Received in revised form 29 January 2011
Accepted 20 February 2011
Available online 26 February 2011

Keywords:
Gasification
Solid oxide fuel cell
Combined heat and power
Exergy

ABSTRACT

A detailed system study on an integrated gasifier–SOFC test system which is being constructed for combined heat and power (CHP) application is presented. The performance of the system is evaluated using thermodynamic calculations. The system includes a fixed bed gasifier and a 5 kW SOFC CHP system. Two kinds of gas cleaning systems, a combined high and low temperature gas cleaning system and a high temperature gas cleaning system, are considered to connect the gasifier and the SOFC system. A complete model of the gasifier–SOFC system with these two gas cleaning systems is built and evaluated in terms of energy and exergy efficiencies. A sensitivity study is carried out to check system responses to different working parameters. The results of this work show that the electrical efficiencies of the gasifier–SOFC CHP systems with different gas cleaning systems are almost the same whereas the gasifier–SOFC CHP systems with the high temperature gas cleaning system offers higher heat efficiency for both energy and exergy.

1. Introduction

Energy systems based on biomass fuels are considered as sustainable because they are practically carbon neutral. Biomass gasification can generate a mixture gas, which is called biosyngas. The biosyngas after purification can be utilized as a fuel in advanced energy systems with gas turbines and/or fuel cells. Within the fuel cell types, solid oxide fuel cells (SOFCs) are being paid much attention because of their advantages like high efficiency and flexibility for different fuels. To use hydrogen, carbon monoxide and methane in the biosyngas for fuelling SOFCs, gas cleaning is necessary. This is to remove contaminants like particulates, tars, sulphur compounds, alkali compounds, and halogen compounds to a level that SOFCs can tolerate, because these contaminants may poison the fuel cells. Different types of gas cleaning technologies are generally suggested to remove those impurities. However, impurity constraints for SOFCs are not clearly understood. General tolerance levels for SOFCs for contaminants within the raw biosyngas and typical gas cleaning options for those contaminants are given in Table 1.

The combination of biomass gasifiers and SOFCs is a subject of many studies. These studies can be divided into several topics like feasibility studies, studies on gasification effects, complete system studies, and studies on safe SOFC operation when fed with biosyngas. Colpan et al. [1] focused on the effects of gasification agents (air, enriched oxygen and steam) on SOFC performance and showed the highest electrical efficiency (41.8%) with steam as the gasification agent. Athanasiou et al. [2] studied the integration of solid oxide fuel cells (SOFCs) in biomass gasification–gas turbine systems for the estimation of the overall electrical efficiency. The effect of the lower heating value of biomass on system performance was analyzed. As for gasifier–SOFC system studies, Aravind et al. [3] did detailed modeling work on gasifier–SOFC–gas turbine hybrid systems. The results show that total (combined heat and power) CHP system efficiency can be over 70%. Omosun et al. [4] employed two different gasifiers and considered cold gas cleaning and hot gas cleaning processes for gasifier–SOFC systems. No significant difference in electrical efficiency was found but a significant deviation (26%) in total CHP efficiency was observed. For safe operation of gasifier–SOFC systems, Mermelstein et al. [5] used benzene to model tar in biomass gasification. They investigated experimentally the impacts of steam and current density on carbon formation on Ni/YSZ and Ni/CGO SOFC anodes. Carbon formation and cell degradation was studied. However, the carbon deposition could be reduced by means of steam reforming of tar over the nickel anode, and partial oxidation of tar while operating the fuel cell under load. Aravind et al. [6] investigated the influence of H_2S, HCl and naphthalene on SOFC Ni-GDC anodes. No significant impact has been observed up to 9 ppm H_2S and HCl and 110 ppm naphthalene in this work. Ouweltjes et al. [7] presented the results of biosyngas utilization in solid oxide fuel cells with Ni-GDC anodes at 850 and

* Corresponding author. Tel.: +31 15 2786987; fax: +31 15 2782460.
E-mail address: ming.liu@tudelft.nl (M. Liu).

0378-7753/$ – see front matter © 2011 Elsevier B.V. All rights reserved.
doi:10.1016/j.jpowsour.2011.02.065

Table 1
SOFC tolerance on contaminants and typical gas cleaning options [15].

Contaminants	SOFC tolerance	Low temperature	High temperature
Particles	Few ppmw	Bag filter, cyclone wet scrubber, wet electrostatic precipitator (WESP)	Cyclone, ESP, bag filter, granular bed filter, rigid barrier filter
Tars	Few ppmw	Wet scrubber, WESP, filter	Cracking with catalysts (750–900 °C), or high temperature thermal (900–1200 °C) cracking
Alkali compounds	Few ppmw	Removal as solid particles	Removal as solid particles (<600 °C), alkali getter (>800 °C)
H_2S	Few ppmv	Wet scrubber, activated carbon,	Sorbents (>300 °C, e.g. ZnO)
HCl	Few ppmv	Wet scrubber	Sorbents (300–600 °C, e.g. Na_2CO_3)

920 °C. The investigations made clear that Ni-GDC anodes can be operated within a wide range of biosyngas compositions. Hofmann et al. [8] investigated the influence of real biosyngas with a tar level over 10 g N m^{-3} on SOFC Ni-GDC anodes reporting successful SOFC operation for 7 h. Planar SOFC operation on real wood gas from the Viking two-stage fixed-bed downdraft gasifier was investigated and smooth operation without carbon deposition and significant performance degradation for 150 h has also been reported in [9]. Besides these, several other studies [10–14] provide more insight into gasifier–SOFC systems.

In this paper, we present the results from detailed thermodynamic evaluations of a gasifier–SOFC test system which is under development. A small scale SOFC CHP system developed by Fuel Cell Technologies Ltd. (FCT) based on tubular SOFCs from Siemens is being integrated with a commercial downdraft fixed-bed gasifier. Two types of gas cleaning systems, a combined high and low temperature gas cleaning system (CTGCS) and a high temperature gas cleaning system (HTGCS), were proposed for this integration. Thermodynamic calculations were first carried out to evaluate the performance of the SOFC system fed by natural gas. Then the performance of the SOFC system fed by biosyngas purified using the proposed gas cleaning systems was evaluated in terms of energy and exergy efficiencies. A sensitivity study was conducted to check system responses to changes in various working parameters and to obtain suitable working conditions for safe system operation and for improved gasifier–SOFC system performance.

2. System configuration

2.1. Gasifier

A downdraft fixed-bed reactor using air (double-stage) as the gasifying agent is employed for the gasifier–SOFC system. This gasifier with the thermal capacity of 50 kW and the electric capacity of 10 kW essentially consists of four sections assembled together. The top section has two parts; an upper cylindrical fuel inlet part and a conical fuel storage part. The second section has a mild steel cylinder with a primary stage for air feed. The third section above the grate serves as the reduction zone where biosyngas is formed. The second stage of air supply is close to the upper part of the third section. The bottom section has an ash pit performing as an ignition port and an ash removal section and the outlet of the production biosyngas. Two vibrators are set on the first and third sections to avoid the formation of bridges resulting in unstable gasification operation.

The gasifier described above is used because of (1) lower particulate levels in the produced gas and (2) lower tar content in the gas because most tars are destroyed by thermal cracking as they pass through the hot reduction zone. The double stage air provision further reduces tar content [16]. Low tar levels in biosyngas from the gasifier will reduce the cleaning load of the downstream tar removal unit. Hence the tar cleaning unit can be built at reduced costs. The gasifier works at ambient pressure and the stable gasification zone temperature is around 750–850 °C. Detailed information and test results on this gasifier are available elsewhere [17].

2.2. Gas cleaning system

2.2.1. Combined high and low temperature

The CTGCS mentioned in this work has both high and low temperature components. The biosyngas which leaves the gasifier first passes a cyclone to eliminate large size particulates and then goes to a ceramic filter by which particulate-free biosyngas can be obtained. Following these two units is a dolomite/nickel catalyst-based tar reformer working around 800 °C, through which the tar within the biosyngas is almost completely decomposed into gases like CO and H_2 [18]. After the steam reforming the gas is fed to a water scrubber, which removes most of the impurities like particles, alkalis, and halogens by cold water. After scrubbing, activated carbon is used to absorb sulphur-compounds and other trace components, which may have escaped the scrubber. Although some water vapor (around 2 vol.% as indicated in the model) in the biosyngas after scrubbing may deactivate a small part of the activated carbon, it is still necessary to ensure a sulphur-free or least possible sulphur containing biosyngas. The cleaned biosyngas at around room temperature then flows to the SOFC system. In this gas cleaning system, waste water, coming from the scrubber, will not contain large amounts of tars. The cost of waste water treatment will be much lower than for the system without the tar reformer. However, the water should be further treated before it can be disposed off [19,20].

2.2.2. High temperature

In the high temperature gas cleaning process as shown in Fig. 1, raw biosyngas first passes through a cyclone and a dolomite/nickel based catalyst reactor working at 800 °C. Then the hot gas is cooled using cold water for producing hot water. The biosyngas is cooled down to around 450 °C under which alkalis are expected to condense on particulates. The particulates together with the condensed alkali compounds are then removed by a primary-stage filter. Then the biosyngas passes through two units working around 450 °C, in which subsequent beds with sodium carbonate and zinc oxide sorbents remove halide and sulphur compounds from the biosyngas. After passing through the second-stage filter, purified biosyngas is then supplied to the downstream SOFC system.

2.3. SOFC CHP system

The SOFC CHP system is based on the Alpha unit developed by Fuel Cell Technologies. The SOFC stack inside the Alpha unit employs the tubular SOFCs developed by Siemens. The stack operates at 900–1000 °C and at close to atmospheric pressure. Generally, desulphurized natural gas as fuel is compressed and fed to an ejector that pulls a part of anode-off gas from a recirculation plenum into the steam reformer. A part of the natural gas is reformed by the recycled steam in the steam reformer. The rest of the gas will be

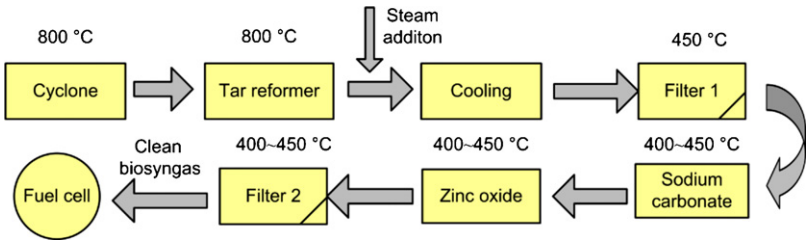

Fig. 1. Flow diagram of the high temperature gas cleaning system.

converted to hydrogen and carbon monoxide by internal reforming. The other portion of the anode-off gas passes to the post-combustor or after burner and reacts with the air from the cathode. A part of the heat from the flue gas leaving the post-combustor is used to preheat the air that goes to the cathode, and the remaining heat in the flue gas is recovered by a heat exchanger for space heating and/or domestic hot water production. The flow scheme of the Alpha unit is presented in Fig. 2. More details about this unit are available in [21].

3. Modeling

3.1. Gasifier

The gasification section in the models built in computer program Cycle Tempo [22] is based on equilibrium calculations. The composition of the produced gas is calculated by minimizing the Gibbs energy. For the equilibrium calculations, the gasifier is considered to be working at a temperature of 800 °C and a pressure close to ambient pressure, and a gas outlet temperature of 800 °C is assumed. A part of the carbon within biomass, around 5% is not converted and is removed from the gasifier representing the losses that usually occur in downdraft fixed-bed gasifiers. Eucalyptus wood is used as the biomass fuel for the gasifier, and its composition taken from the Phyllis database [23] is given in Table 2. The methane concentration was adjusted to fit experimental data in the gasifier model as explained elsewhere [3].

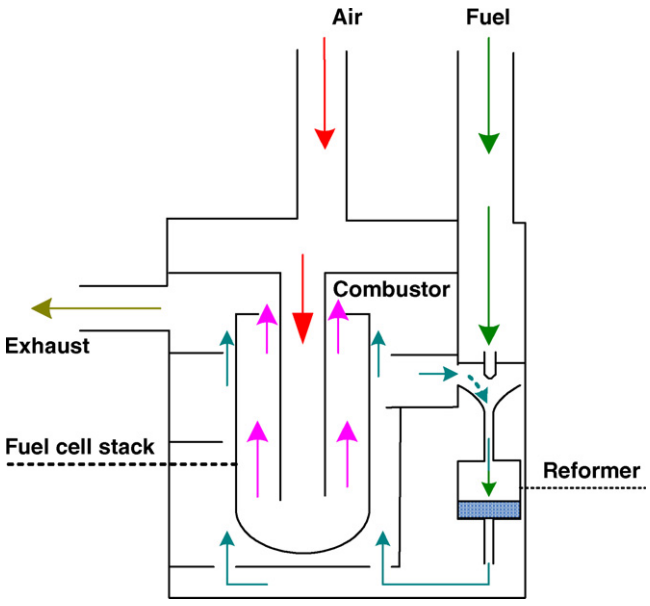

Fig. 2. Flow scheme of the SOFC system.

3.2. Anode recirculation

In the model a recirculation fan (NO.110 in base case, NO.117 in case 1 and NO.118 in cases 2 and 3) is employed to simulate the functions of the ejector in the Alpha unit. The ejector is an important component as it (1) compensates pressure losses in the anode chamber of the fuel cell stack, and (2) recirculates the anode-off gas which is steam rich and supplies sufficient steam to support the reforming taking place in external reformer. In all cases presented in this work, the anode recirculation fraction is determined by avoiding the risk of carbon deposition as discussed in Section 4.3.

3.3. Gas processing

The calculations for the steam reformer and combustor in the systems are based on the minimization of the Gibbs free energy. Natural gas and other higher hydrocarbons would have steam reforming described by Eq. (1) and water gas shift reaction described by Eq. (2), which are considered to be in equilibrium.

$$C_xH_y + xH_2O \leftrightarrow xCO + ((2x+y)/2)H_2 \quad (1)$$

$$CO + H_2O \leftrightarrow CO_2 + H_2 \quad (2)$$

In the combustor, the remaining fuel in the anode-off gas is oxidized with the cathode-off gas and equilibrium composition is assumed. Flue gas compositions, released heat, mass flows of fuel, oxidant and flue gas can be calculated by the program. Since the contaminants are not actually modeled, the gas cleaning system is mainly accommodated with heat transfer and pressure drops in the gasifier–SOFC CHP systems.

3.4. Fuel cell model

Detailed descriptions of the fuel cell model are available elsewhere [3,22]. It is outlined for the case considered here. The model first takes the inlet gas to the equilibrium conditions. Then, the cell voltage V, the current flow I and the electrical output power P_e are calculated. It is supposed that the processes occur at a constant temperature and pressure. Gas compositions are also supposed to be constant in a cross-section, perpendicular to the direction of the

Table 2
Wood composition in the model.

	Amount	Unit
Carbon (C)	49.5	wt%
Hydrogen (H)	5.75	wt%
Nitrogen (N)	0.14	wt%
Oxygen (O)	44	wt%
Sulphur (S)	0.03	wt%
Chorine (Cl)	0.055	wt%
Lower heating value (dry)	17,963	kJ kg^{-1}

fuel cell flow. A set of equations were used in the fuel cell modeling and they are given below.

$$I = 2F\frac{U_F \Phi_{m,a,in}}{M_a} \times (y^0_{H_2} + y^0_{CO} + 4y^0_{CH_4}) \quad (3)$$

$$V_{rev,x} = V^0_{rev} + \frac{RT}{2F}\ln\left(\frac{y^{1/2}_{O_{2,C}} y_{H_2,a}}{y_{H_2O,a}} \times P^{1/2}_{cell}\right) \quad (4)$$

$$i_x = \frac{I}{A} \quad (5)$$

$$\Delta V_x = i_x \times R_{eq} \quad (6)$$

$$V = V_{rev,x} - \Delta V_x \quad (7)$$

$$P_e = V \times I \times \eta_{DC/AC} \quad (8)$$

Here $\Phi_{m,a,in}$ is the mass flow that goes to the anode (kg s^{-1}), y^0_i are the concentrations at the anode inlet (i is a specie of H_2, CO and CH_4), M_a is the mole mass of the anode gas (kg mol^{-1}), F is the Faraday constant (C mol^{-1}), U_F is the fuel utilization, $V_{rev,x}$ is the reversible voltage (V), V^0_{rev} is the standard reversible voltage for hydrogen (V), i_x is the current density (mA cm^{-2}), R_{eq} is the equivalent resistance (Ω cm^2), ΔV_x is the voltage loss (V), T is the working temperature of the fuel cell stack (K), R is the universal gas constant (J mol^{-1} K^{-1}), P_{cell} is the operating pressure of the fuel cell stack (Pa) and $\eta_{DC/AC}$ is the efficiency of the DC/AC inverter.

3.5. Energy and exergy efficiency

Exergy calculations can be performed using Cycle-Tempo. Exergy analysis allows a system to be analyzed more comprehensively by determining where exergy is destroyed by internal irreversibilities and by bringing out the causes of those irreversibilities. Kinetic and potential exergy effects are neglected. Thermomechanical exergy and chemical exergy are calculated with a reference environment, which is set at a temperature of 15 °C, a pressure of 101,325 Pa with an air composition of Ar 0.91%, CO_2 0.03%, H_2O 1.68%, N_2 76.78%, and O_2 20.60%. The energy efficiencies are calculated based on the lower heating value (LHV) of the fuel. The net AC electrical efficiency, described by Eq. (9), is the ratio of the net produced electricity divided by the mass of the fuel input to the gasifier times the lower heating value. Heat efficiency, described by Eq. (10), is defined as the value of the produced heat divided by the total fuel heating value. Total CHP efficiency is defined as the energy content of products, electricity and heat, divided by the total fuel heating value described by Eq. (11).

$$\eta_{E_{ele}} = \frac{E_{ele} - E_a}{M_{biomass\ \ fuel} \times LMV_{biomass\ \ fuel}} \quad (9)$$

$$\eta_{E_{heat}} = \frac{E_{heat}}{M_{biomass\ \ fuel} \times LMV_{biomass\ \ fuel}} \quad (10)$$

$$\eta_{CHP} = \frac{E_{heat} + E_{ele} - E_a}{M_{biomass\ \ fuel} \times LHV_{biomass\ \ fuel}} \quad (11)$$

E_a is the total power consumption of auxiliary components including compressors and pumps (kW), $M_{biomass\,fuel}$ is the mass flow of the biomass fuel fed to the system (kg s^{-1}), $LHV_{biomass\,fuel}$ is the low heating value of the biomass fuel (kJ kg^{-1}).

Exergy efficiency is defined as the ratio between the exergy of the products and the fuel input exergy. Heat exergy efficiency is described by Eq. (12) and net electricity exergy is given by Eq. (13). System total exergy efficiency is the sum of heat and net electricity exergy efficiency and is described by Eq. (14).

$$\eta_{E_{x,heat}} = \frac{E_{x,heat}}{M_{biomass\ \ fuel} \times E_{x,biomass\ \ fuel}} \quad (12)$$

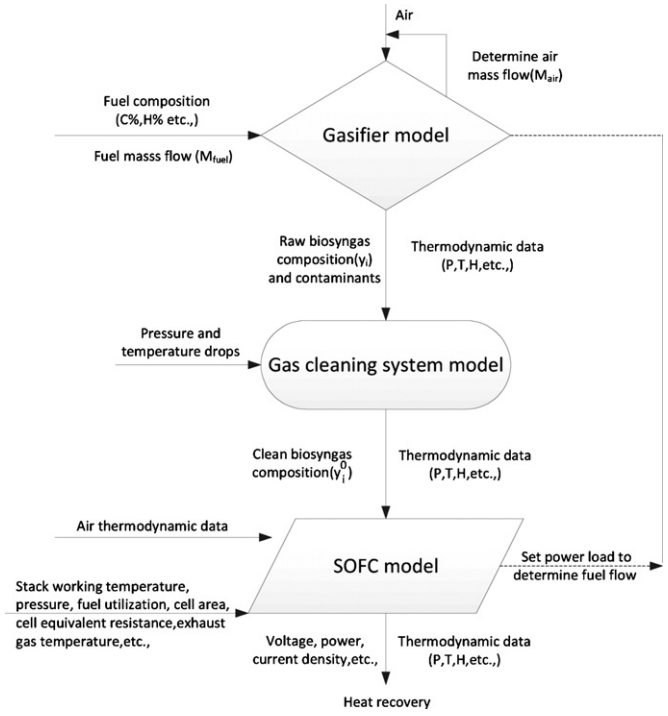

Fig. 3. Flow scheme of the system performance modeling.

$$\eta_{E_{x,ele}} = \frac{E_{x,ele} - E_{x,a}}{M_{biomass\ \ fuel} \times E_{x,biomass\ \ fuel}} \quad (13)$$

$$\eta_{E_{x,CHP}} = \frac{E_{x,heat} + E_{x,ele} - E_{x,a}}{M_{biomass\ \ fuel} \times E_{x,biomass\ \ fuel}} \quad (14)$$

$E_{x,a}$ is the total exergy loss caused by auxiliary components (kJ kg^{-1}), $E_{x,biomass\,fuel}$ is the exergy of the biomass fuel fed to the system (kJ kg^{-1}).

3.6. System modeling process

They are two ways to start the iteration in the program. One way is to specify the biomass fuel mass flow, the other way is to set the power output load of the fuel cell stack. Input and output variables for the system calculation and flow scheme of the whole system modeling are shown in Fig. 3.

3.7. Natural gas fuelled SOFC CHP system (base case)

A simplified model of the SOFC system based on the Alpha unit was built using Cycle-tempo and is shown in Fig. 4. Three heat exchangers are used here to represent the heat transfer within the SOFC system. Some other assumptions are also made for the model, like: (1) the system is under steady state operation, (2) processes are adiabatic, (3) fouling caused by the contaminants on the wall and catalyst is neglected, (4) heat exchangers are supposed to operate in counter flow and (5) pressure drop in all the equipments are estimated. These assumptions are also applied in the cases 1–3 which are described in Section 3.8.

Natural gas is the fuel for the Alpha unit, although several other kinds of gases could be used for the unit if there are appropriate modifications [24]. Since detailed working conditions from experiments with the Alpha unit are not available, the input parameters given in Table 3 are selected from and/or assumed based on other SOFC system calculations performed by Campanari [25] and personal communications [24]. Fresh fuel entering the ejector will be preheated to 700 °C by heat exchange with flue gas in the heat exchanger NO.104 in the model.

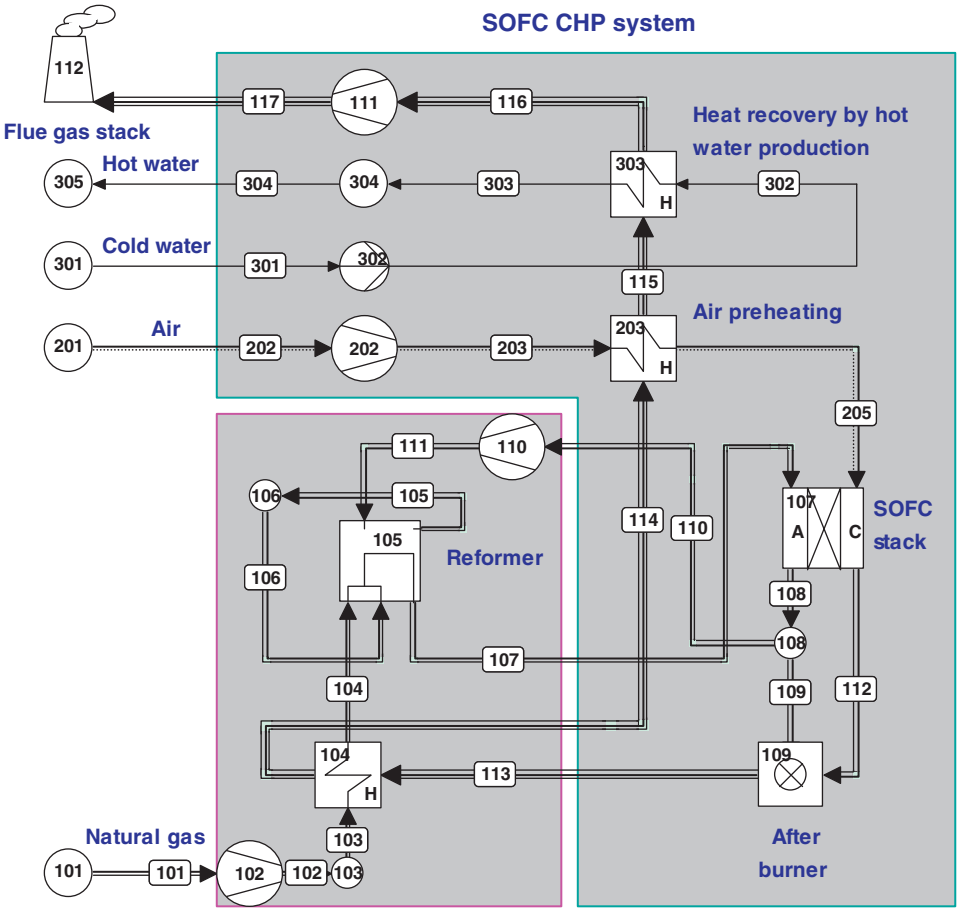

Fig. 4. Flow diagram of the SOFC CHP system fuelled by natural gas (base case).

3.8. Biosyngas fuelled SOFC CHP system

The flow diagrams of SOFC CHP system fuelled by biosyngas which is purified by the two types of gas cleaning systems are shown in Figs. 5–7. The difference between the system shown in Fig. 6 being the case 2 and the one shown in Fig. 7 being the case 3 is the method used for steam generation. The generated steam was added into the biosyngas stream to prevent carbon formation as discussed in Section 4.3. In the case 2, the steam is generated using heat from a combustor fuelled by raw biosyngas, while in the case 3, the steam is provided using heat from the flue gas which exits the post-combustor of the Alpha unit itself. For the case 3, a heat exchanger is required for the extra steam generation and the heat exchanger is placed after the air preheater (NO.124 in Fig. 7) for this purpose. If modifications can be made with the Alpha unit to fulfill this requirement, the case 3 described here may become available. This system gives a higher AC electrical efficiency than that in the case 2. The explanations for this difference are given in Section 4.4.

Table 3
Parameters value used in the SOFC CHP unit calculations.

Parameters	Value
Isentropic efficiency for compressors, blowers and pumps	75%
Mechanical efficiency for compressors, blowers and pumps	98%
Air preheating temperature	993 K
Fuel cell exhaust gas temperature	1183 K
Fuel cell working temperature	1243 K
DC/AC conversion efficiency	92%
Equivalent cell resistance	0.65 Ω cm^2
Cell number	88
Single cell active area	370 cm^2
Global fuel utilization	80%
$\Delta P/P$ air side/fuel side/combustor	0.02/0.03/0.03 bar
Natural gas: CH_4 81.29%, C_2H_6 2.87%, C_3H_8 0.38%, C_4H_{10} 0.15%, C_5H_{12} 0.04%, C_6H_{14} 0.05%, CO_2 0.89%, N_2 14.32%, O_2 0.01%	

4. Results

4.1. Gasification

The input composition of the biomass used for gasification is given in Table 2 and the results from the model calculations are given in Table 4. The biosyngas composition obtained from the calculation generally matches well with the experimental data, except for carbon dioxide. CH_4, H_2, and CO was measured experimentally, while other gases were calculated based on mass and energy balance [17], which may be the reason for this deviation. Generally, as the product compositions from the gasifier model are in reasonable agreement with the experimental data and it is expected that

Table 4
Gas composition comparison.

Component	Model (vol.%)	Experiment (vol.%)
CH_4	1.35	0.8–2
H_2	15.94	12–17
H_2O	9.72	9–11
N_2	40.66	40–44
CO_2	11.32	13–16
CO	17.04	14–22

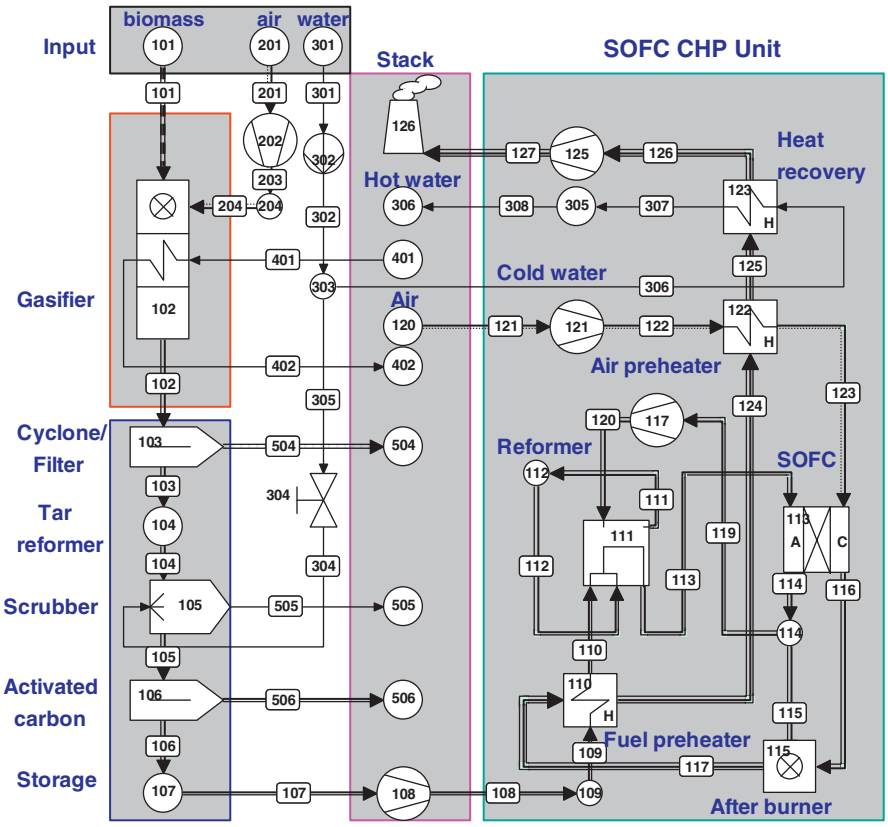

Fig. 5. Flow diagram of the gasifier–CTGCS–SOFC CHP system (case 1).

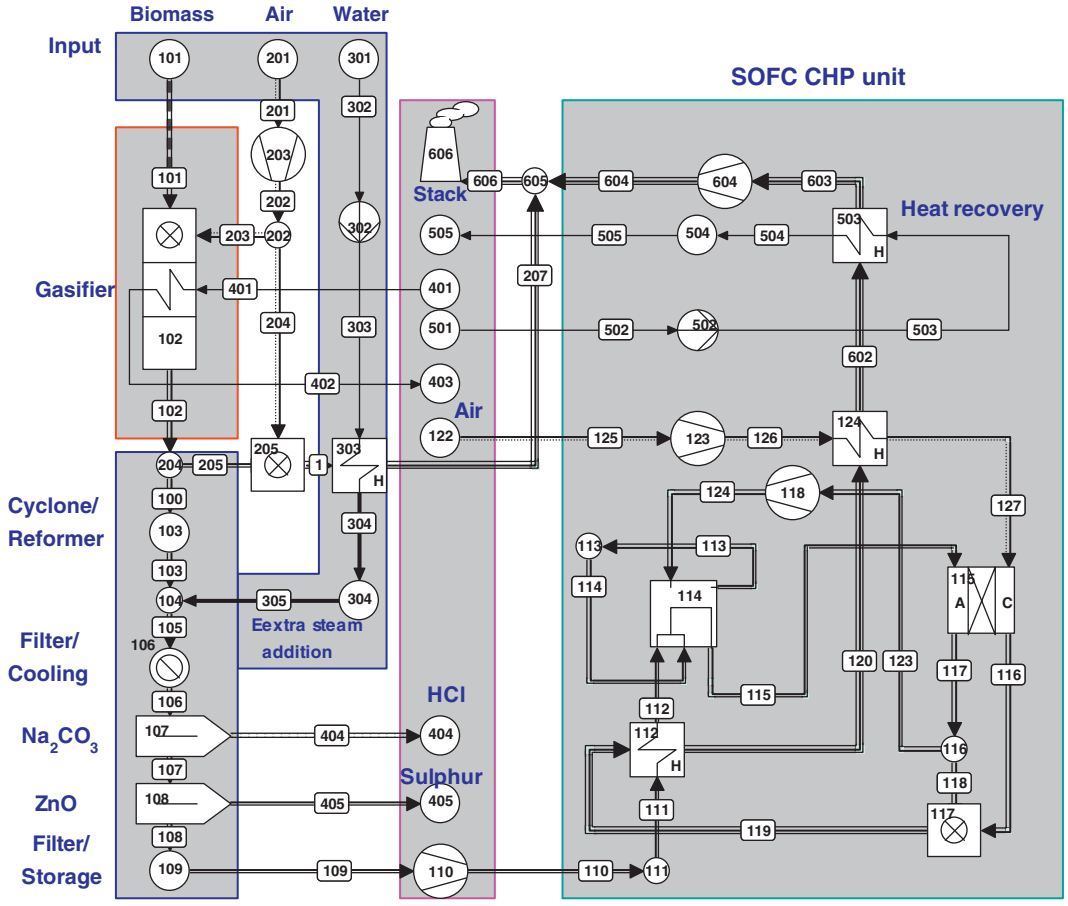

Fig. 6. Flow diagram of the gasifier–HTGCS–SOFC CHP system with external combustor for extra steam generation (case 2)

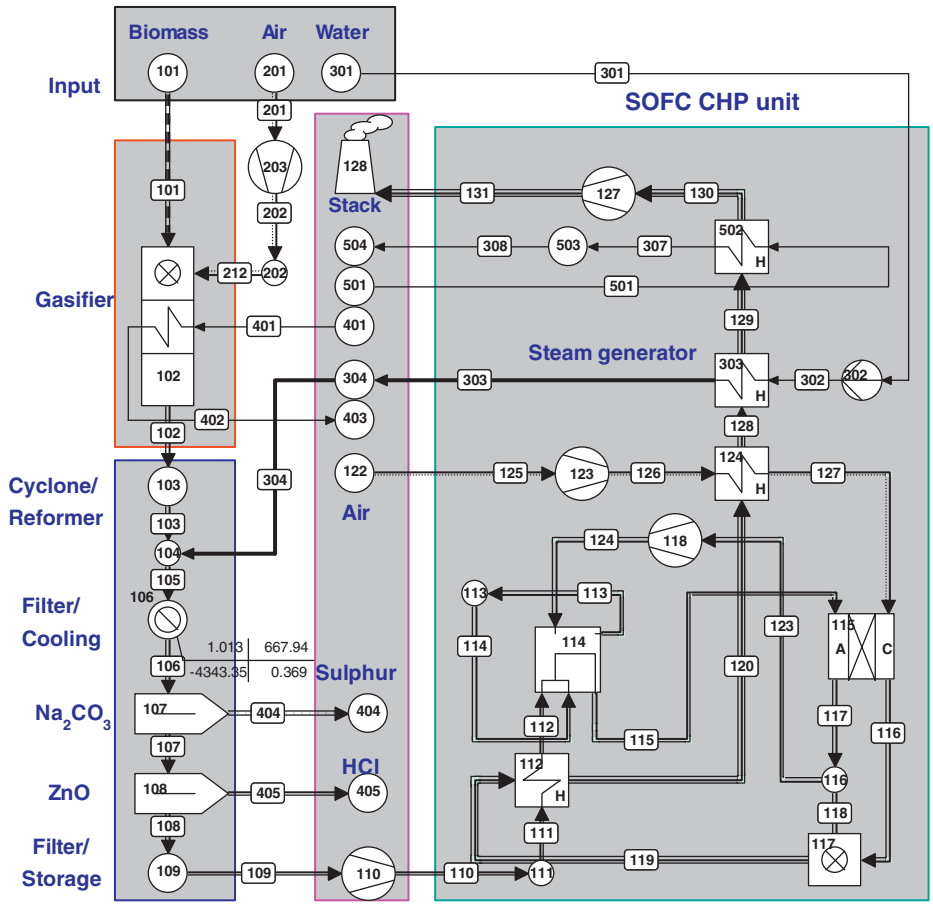

Fig. 7. Flow diagram of the gasifier–HTGCS–SOFC CHP system with internally modified section for steam generation (case 3)

deviation in CO_2 does not influence system performance too much, this gasification model is considered acceptable and is used for the performance evaluation of the gasifier–SOFC systems.

4.2. Fuel cell model validation

For a single tubular SOFC, also developed by Siemens, the behavior in terms of current–density to voltage and current–density to power–density is calculated using the fuel cell model in Cycle-Tempo. The results are compared with experimental results from [26] and the comparison is shown in Fig. 8. The single cell is working at 900 °C and the inlet fuel consists of 89% hydrogen and 11% water vapor. Fuel utilization is set to 85% in the model. The maximum difference between modeling and experimental values is less than 4%, showing a fairly good fit and indicating the proposed model works reasonably well to predict the performance of the tubular SOFC.

4.3. Carbon deposition

Carbon deposition can cause blocking of the gas pipes, system performance degradation and even anode damage. In the C–H–O diagram, when gas composition lies below the carbon deposition boundary, no solid carbon exists, and if the gas composition lies above the curve, carbon formation will occur [3]. The possible sections where carbon deposition may happen are analyzed based on thermodynamic calculations using Factsage 5.4.1 [27] and the ternary diagram indicating carbon deposition is shown in Fig. 9.

In the base case, the gas composition of the natural gas is represented by point A in the ternary diagram. It is located at the carbon deposition region of all carbon boundary lines of different working temperature levels in the diagram. Natural gas with a part of recycled anode-off gas, represented by point B, in the steam reformer is far away from the carbon boundary line at 600 °C as indicated in the diagram.

In the case 1, as the gas is cooled fast in the scrubber, the chemical reactions causing carbon deposition are not expected to take place at ambient temperature. Even if solid carbon is formed, most of it is likely to get removed in the scrubber. The biosyngas mixed with anode-off gas in the steam reformer working at 600 °C and

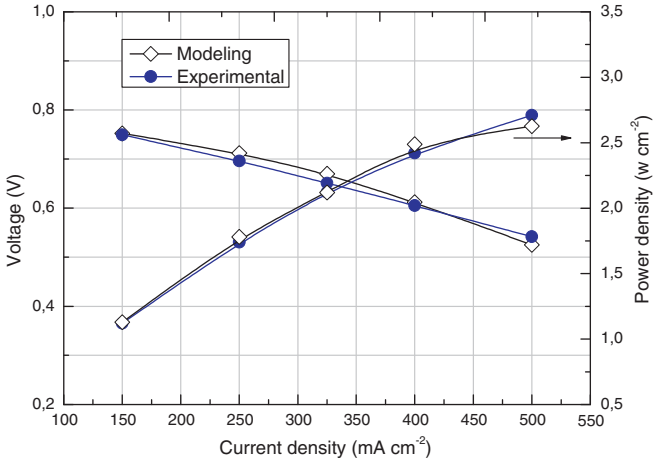

Fig. 8. Experimental and modeling data of a single cell at 900 °C under 89% H_2 and 11% H_2O

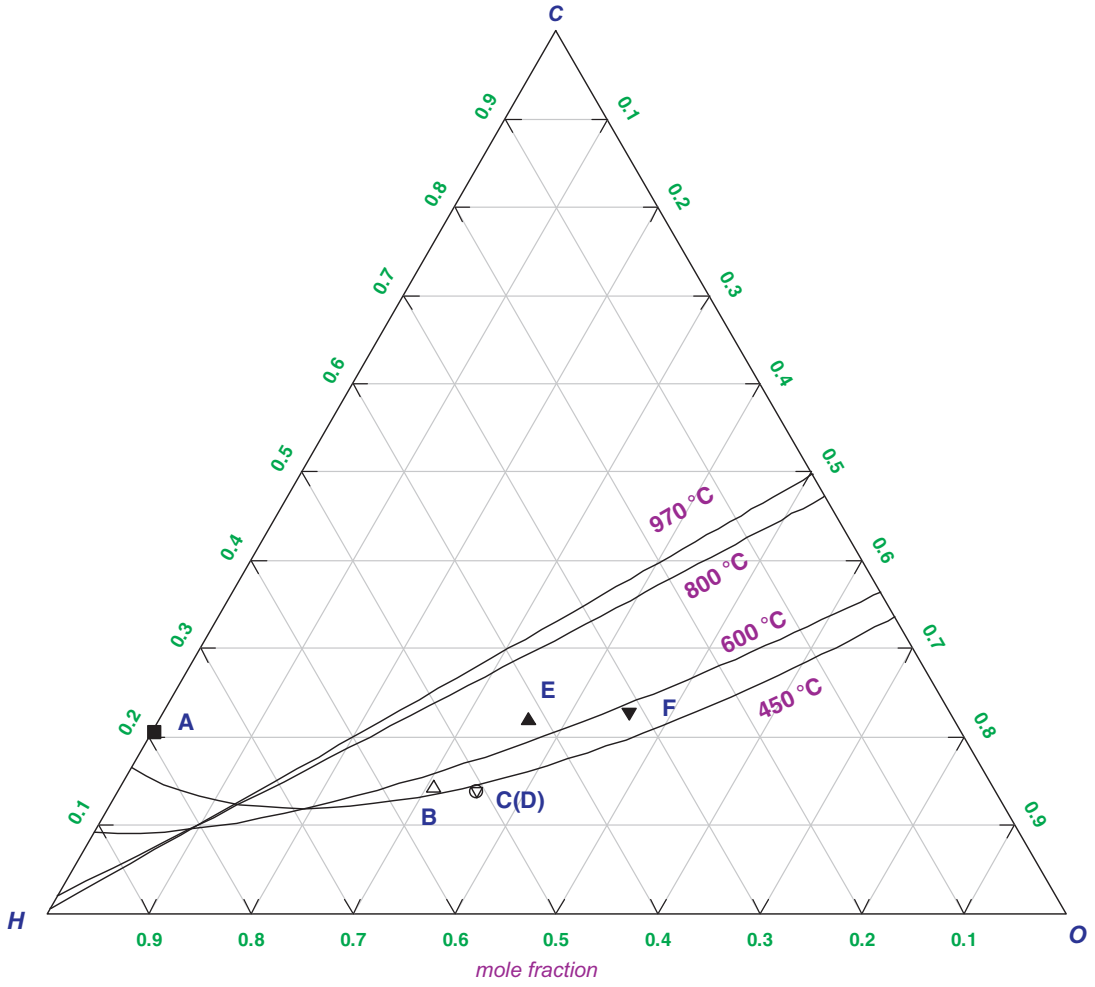

Fig. 9. C–H–O ternary diagram indicating carbon deposition region (A represents the natural gas, B represents the natural gas with recycled anode-off gas in base case, F represents biosyngas with recycled anode-off gas in case 1, C represents biosyngas with steam added in cases 2 and 3, D represents biosyngas with recycled anode-off gas in cases 2 and 3, E represents raw biosyngas, 970 °C is fuel cell stack working temperature, 800 °C and 600 °C is the temperature of raw biosyngas and steam reformer, respectively, 450 °C is the biosyngas after cooling in cases 2 and 3, note: there is an overlap between points C and D).

ambient pressure is in the carbon free region as point F is below the carbon formation boundary line at this temperature.

In the cases 2 and 3, when the biosyngas is cooled down from 800 to 450 °C, carbon formation may occur as point E is located above the carbon boundary line at 450 °C; therefore, steam addition is required. About 17% steam (by volume of biosyngas) is added into gas mainstream which makes the biosyngas escape from the carbon deposition region from point E to point C. Since the anode-off gas will bring steam rich gas to the steam reformer, this will drag point C further away from the carbon boundary, hence no carbon is expected to be formed in the steam reformer.

It must be noted is that thermodynamic calculations only give indications regarding the carbon deposition while other factors such as kinetics will also influence it. For example, Mermelstein et al. [28] found carbon deposition on SOFC anodes even with a steam to carbon ratio >1, which is not favourable for carbon formation as indicated in thermodynamic calculations. Further studies are required to arrive at solid conclusions for preventing carbon deposition in the gasifier–SOFC systems.

4.4. System performance

The performance of the SOFC CHP system with regard to energy conversion for all the considered cases is given in Table 5. The SOFC CHP system fuelled by the natural gas presented here has a larger deviation in the performance compared to that from literature [29]. This deviation may arise from the assumptions related to the balance of plant (BOP), deviation in working conditions and natural gas composition. Normally, electrical power of the Alpha unit is usually de-rated by 30–35% [21] caused by BOP, especially by poor efficiency of DC/AC inverter in real operations. The electrical efficiency changes to 39.8% if the inverter efficiency decreases from a theoretical value of 92% to 75%, a typical value in operation. This shows good agreement with the value from the literature [29]. The thermal efficiency appears to be higher than that from the literature; this may be caused by the lower temperature (100 °C in this work) of the exhaust flue gas, which is typically in the range of 100–200 °C in real operations. The adiabatic assumption also has an influence on the thermal efficiency. Exergy efficiencies for net

Table 5
SOFC CHP system energy conversion performance.

	Base case	Case 1	Case 2	Case 3
Fuel input (kW)	9.12	18.43	18.43	18.43
AC power output SOFC (kW)	4.65	4.61	4.25	4.59
Heat output (kW)	3.48	6.24	8.18	7.69
Auxiliary consumption (kW)	0.16	0.35	0.27	0.28
Gross electrical efficiency (%)	50.9	25.0	23.0	24.9
Net AC electrical efficiency (%)	49.2	23.1	21.6	23.3
Heat efficiency (%)	38.1	33.9	44.4	41.7
CHP efficiency (%)	87.4	57.0	66.0	65.0

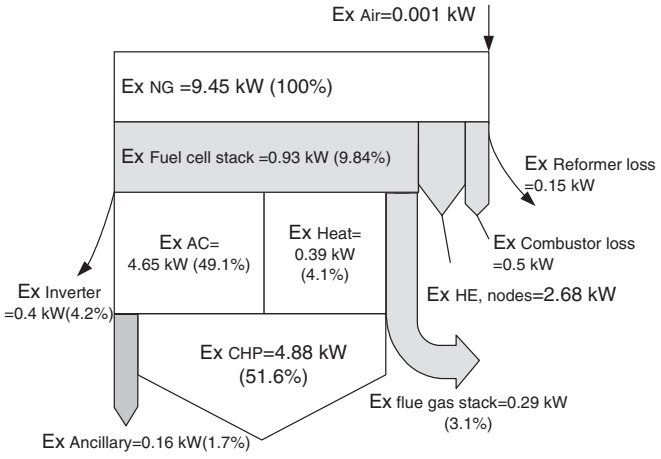

Fig. 10. Exergy flow diagram of base case.

AC electricity and heat are around 47.5% and 4.1%, respectively in the calculations, and the exergy flow diagram is plotted in Fig. 10. Around 62% of the anode-off gas is recirculated, which makes it thermodynamically unlikely that carbon deposition will occur in the external reformer and in the anode as discussed in Section 4.3.

In the gasifier–SOFC systems (cases 1–3), for a mass flow of biomass fuel (0.00114 kg s^{-1}), the gross AC electrical efficiency is higher in the case 1 than in the cases 2 and 3 (no modifications were made on the electrical efficiency as previously explained for the base case). This can be explained by the difference in steam concentration as the steam content of the fuel gas is lower in the case 1 while extra steam addition for suppressing carbon deposition in the cases 2 and 3 reduces the electrical efficiency. Parasitic power in the cases 1–3 does not show much difference, but the cases 1 and 3 which have different gas cleaning systems give comparable electrical efficiencies which are slightly higher than that in the case 2. It is clearly seen that thermal efficiencies in the cases 2 and 3 with the HTGCS are almost 9% higher than that in the case 1 with the CTGCS, this is because of the lower heat losses in the systems with HTGCS. In this regard, CTGCS is proposed for integration in a gasifier SOFC system when electricity production is given importance, and HTGCS may be preferred when there is a high heat demand. However, when considering the maturity of gas cleaning technologies and cost effectiveness, CTGCS shall be initially preferred for the gasifier–SOFC systems. An interesting point is the performance difference between the cases 2 and 3 caused by different means of steam generation to avoid the risk of carbon formation. Since a split stream of raw biosyngas fuel is used as the fuel for the extra combustor in the case 2 to produce steam from cold water, less fuel flows to the SOFC system generating less electricity which causes a lower electrical efficiency. However, the case 2 has around 3% higher thermal efficiency than the case 3, this is mainly because in the case 3 less heat can be recovered in the case 3 as more heat is needed for steam generation in this case.

The exergy flows in the gasifier–SOFC CHP systems, i.e. the cases 2–4 are shown in Figs. 11–13, respectively (HE in the plot stands for heat exchanger). It is found that the gasification process causes the largest exergy loss, which is about 24% of the system input exergy. This exergy loss is mainly caused by the large irreversibilities including the heating of the cold fuel and air, combustion, gasification, and carbon losses, which occur during the gasification process. The exergy losses of the gas cleaning process are not significant due to the low content of impurities and also small pressure and temperature drops. However, due to the larger temperature drop in the case 1 with the combined high and low temperature gas cleaning process compared to that in the cases 2 and 3 with high temperature gas cleaning technologies, the exergy loss of the gas cleaning system is higher in the former case. For the SOFC CHP system, the fuel cell stack causes only a small part of the total exergy losses. For the complete system, the case 3 shows the highest system exergy efficiency of 28.1% among three cases mainly because more heat was recovered. However, no significant difference in electricity exergy efficiency is found in these three cases. The exergy performance of all the cases is summarized in Table 6.

Table 6
SOFC CHP system exergy performance.

	Base case	Case 1	Case 2	Case 3
Fuel exergy input (kW)	9.45	20.76	20.76	20.76
AC power output SOFC (kW)	4.65	4.61	4.25	4.59
Heat output (kW)	0.39	0.69	1.52	1.53
Auxiliary consumption (kW)	0.16	0.35	0.27	0.28
Gross electricity exergy efficiency (%)	49.1	22.2	20.4	22.1
Net AC electricity exergy efficiency (%)	47.5	20.5	19.2	20.7
Heat exergy efficiency (%)	4.1	3.3	7.3	7.4
CHP exergy efficiency (%)	51.6	23.9	26.5	28.1

4.5. System performance responses to variation in parameters

To safely operate the SOFC system using the biosyngas in order to partly or completely replace natural gas, and to obtain high system efficiency, suitable off-design working conditions need to be explored. For the fixed-bed downdraft with air as the gasifying agent and wood as the fuel employed here, the gasifier performance is relatively stable. During experimental work on the gasifier, it is found that the moisture content in the wood has a large effect on the system performance. The wood was dried naturally and therefore the moisture content depends heavily on the weather condition and drying time. It can be expected that the gasification efficiency and SOFC system performance would drop if biomass with high moisture content was used, because then more biomass fuel will be necessary to evaporate the additional moisture before gasification. This decreases the fuel flows to the SOFC and less power can be generated. Generally, for a gasification based power generation system, biomass moisture content should be below 10–20% as pointed in [30]. The level of contaminants like tars and sulphur-compounds in the product biosyngas also has a great influence on SOFC performance. However the gas cleaning process described here is not actually modeled. It is expected that the gas cleaning systems can reduce the contaminants to sufficiently low concentrations in the biosyngas that they do not affect the SOFC performance, hence working parameters of the gas cleaning process are not further discussed. In this work, we focus our sensitivity analysis on the SOFC system and the system of case 1 is employed for this study.

4.5.1. Influence of fuel utilization

Fuel utilization is one of the main operation parameters of the SOFC system. It determines the composition of the anode exhaust gas which is recirculated and hence influences the carbon formation that can occur in the downstream steam reformer. Moreover, fuel utilization usually cannot be more than 85%; higher values will result in a performance drop of the SOFC. This drop is due to several reasons such as gas composition changes or formation of nickel oxide [31]. For real biosyngas fuelled SOFCs, many experiments [32,11] use low fuel utilization down to 20% in order to have a safe working condition to protect the cell. In [11], it is found that high fuel utilization (75%) caused a SOFC performance loss because of nickel oxidation on Ni-GDC anode. On the contrary, literature [33] shows that a fuel utilization of about 75% is possible with syngas produced from gasification in a commercial SOFC stack with Ni-CGO anodes [34]. Considering these, fuel utilization in the range

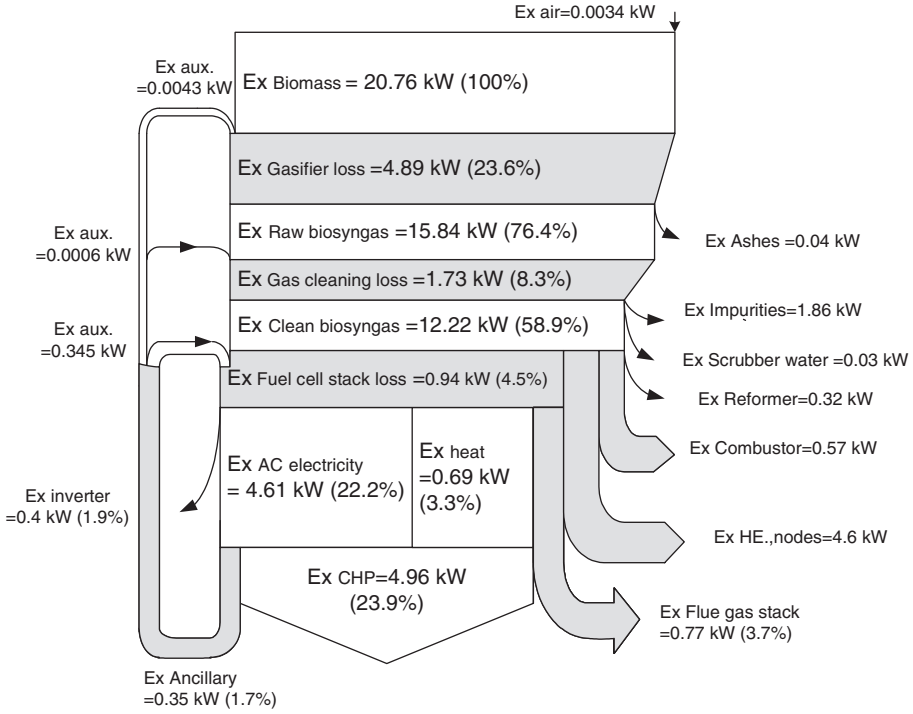

Fig. 11. Exergy flow diagram of case 1.

of 65–85% is selected for the sensitivity study in the gasifier–SOFC system of the case 1 employed here.

Fig. 14(a) reveals the relationship between variable fuel utilization and system energy conversion performance under a certain biomass flow rate. Apparently, the electrical efficiency increases with increasing fuel utilization because more power is produced when recirculation rate is around 60%, as shown in Fig. 14(a). Higher fuel utilization induces less fuel go to the combustor and hence less heat can be recovered. The total CHP efficiency also increases with increasing fuel utilization because the increase of electrical efficiency is higher than the decrease of heat efficiency. The thermal efficiency is less influenced by the fuel utilization than the electrical efficiency. It seems that the total CHP efficiency reaches to a maximum value at around 80% in this case. The system exergy performance as a function of the fuel utilization is shown in Fig. 14(b). Since the net AC power output increases with increasing fuel utilization, the net AC electricity exergy efficiency increases too. The heat exergy efficiency decreases with increasing fuel utilization,

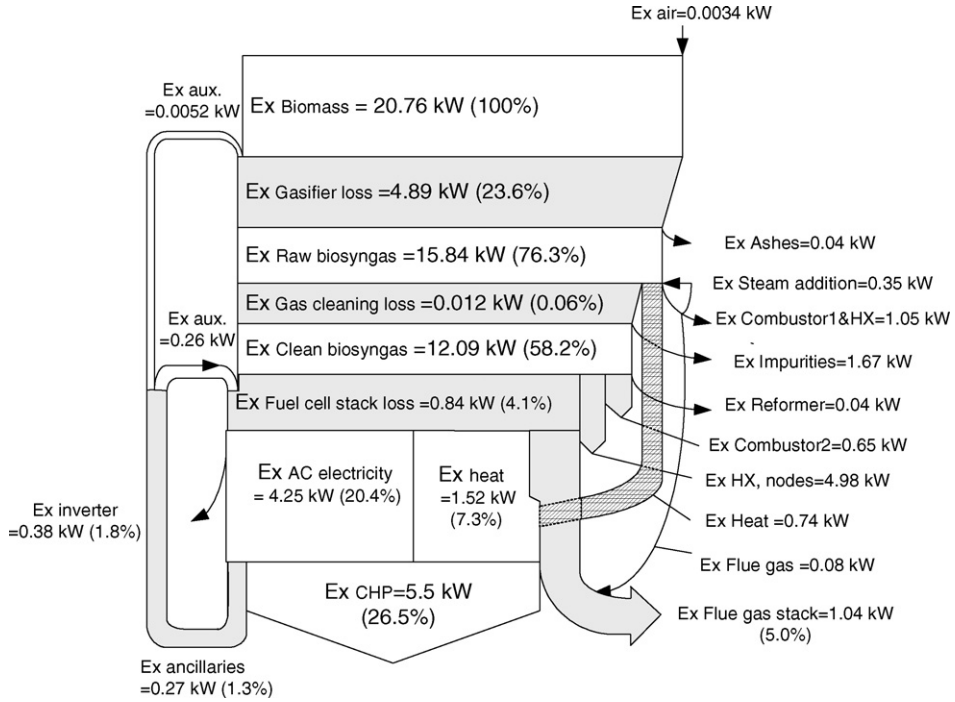

Fig. 12. Exergy flow diagram of case 2.

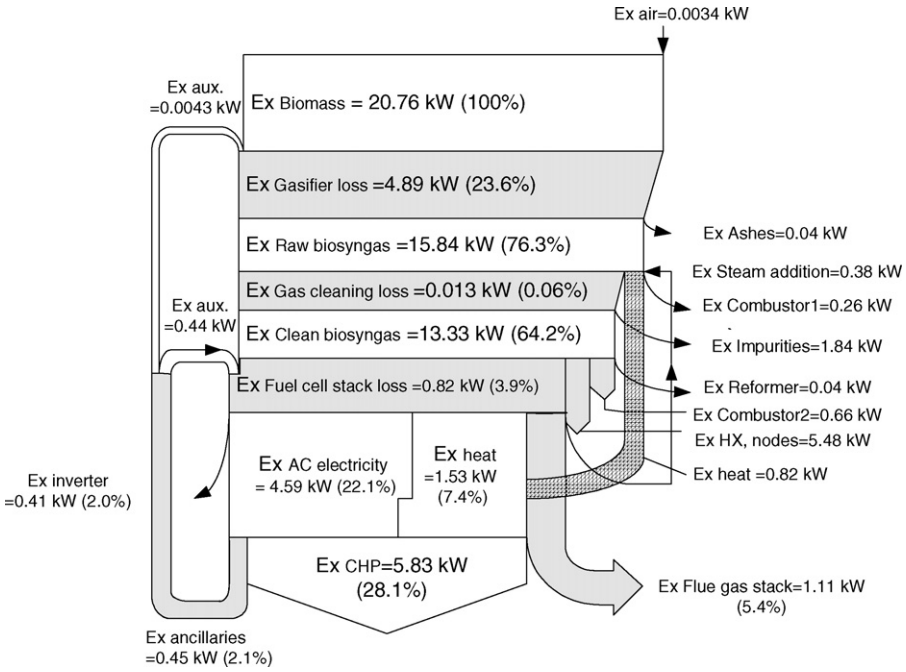

Fig. 13. Exergy flow diagram of case 3.

but it does not have too much influence on system CHP exergy efficiency which is higher for higher fuel utilization. For all the calculations with regard to the influence of fuel utilization, carbon deposition-free operation conditions for the steam reformer and the fuel cell stack were carefully checked and adjusted in the program using the C–H–O ternary diagram, especially for the conditions of lower fuel utilization as these conditions have lower steam levels but higher CO concentrations.

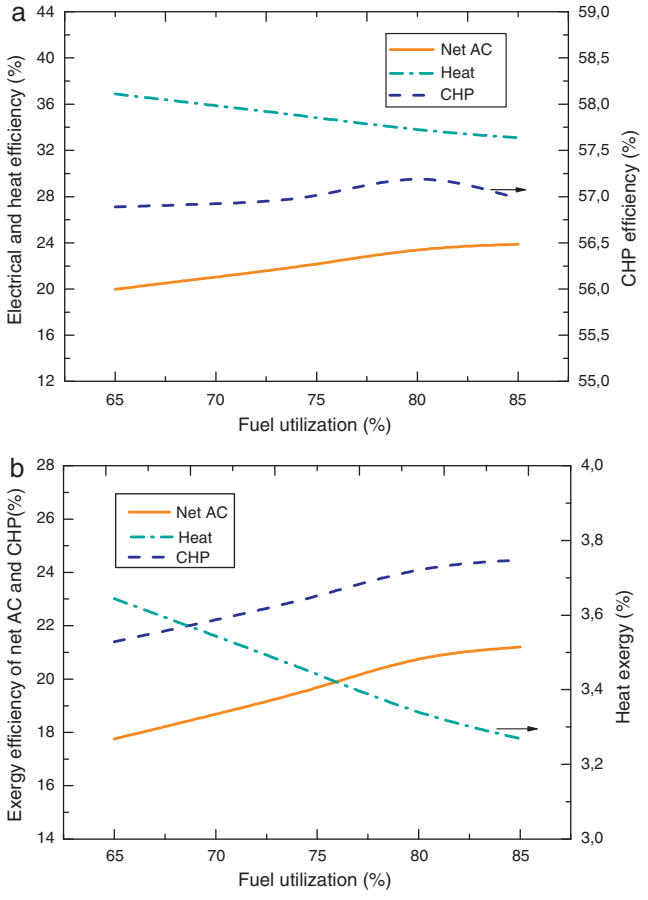

Fig. 14. (a) Effect of fuel utilization on energy conversion efficiency and (b) effect of fuel utilization on system exergy efficiency.

4.5.2. *Influence of current density*

In real operation of the fuel cell stack, stack current is directly controllable. Current density can be varied in the model when fixing other parameters as listed in Table 3. Fig. 15(a) demonstrates the changes in electrical and thermal cogeneration efficiency when varying the current density. It is evident that electrical efficiency decreases with increasing current density due to increased polarization losses. The decreased cell voltage degrades the stack performance under the constant fuel utilization. A decreased electrical efficiency of the fuel cell stack means that more chemical energy is transformed into heat; hence more heat can be recovered. The system CHP efficiency slightly decreases but it does not change too much. The exergy efficiency of the system, shown in Fig. 15(b) has a similar changing trend as energy conversion efficiency.

4.5.3. *Influence of anode recirculation*

Anode recirculation plays an important role in the system as it not only prevents carbon formation in the external reformer and in the anode chamber but it also influences the anode fuel inlet temperature which might have an impact on the thermal stresses within the fuel cell stack.

Since the concentration of methane in the biosyngas is very low and the anode-off gas is rich in water vapor, it is not necessary to have a higher anode recirculation ratio; the higher anode recirculation dilutes the fresh fuel which decreases the fuel cell net AC electrical efficiency although system heat efficiency slightly increases. The influence of the anode recirculation on system energy and exergy efficiency can be clearly seen from Fig. 16. It is also found that the temperature of reformate gas exiting the external reformer increases with increasing the anode recirculation fraction. Although it helps to reduce the thermal gradient of the fuel cell stack to some extent, it also reduces the system net AC efficiency. In this regard, a lower anode recirculation ratio which fulfills the requirement of steam for supporting the external reforming

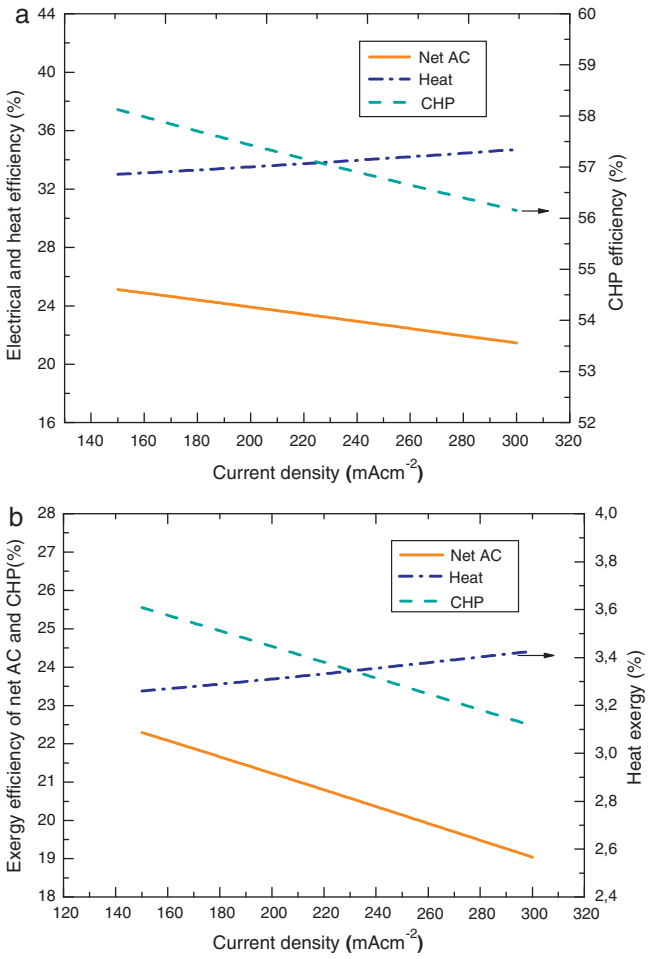

Fig. 15. (a) System energy conversion as a function of current density and (b) system exergy performance as a function of current density.

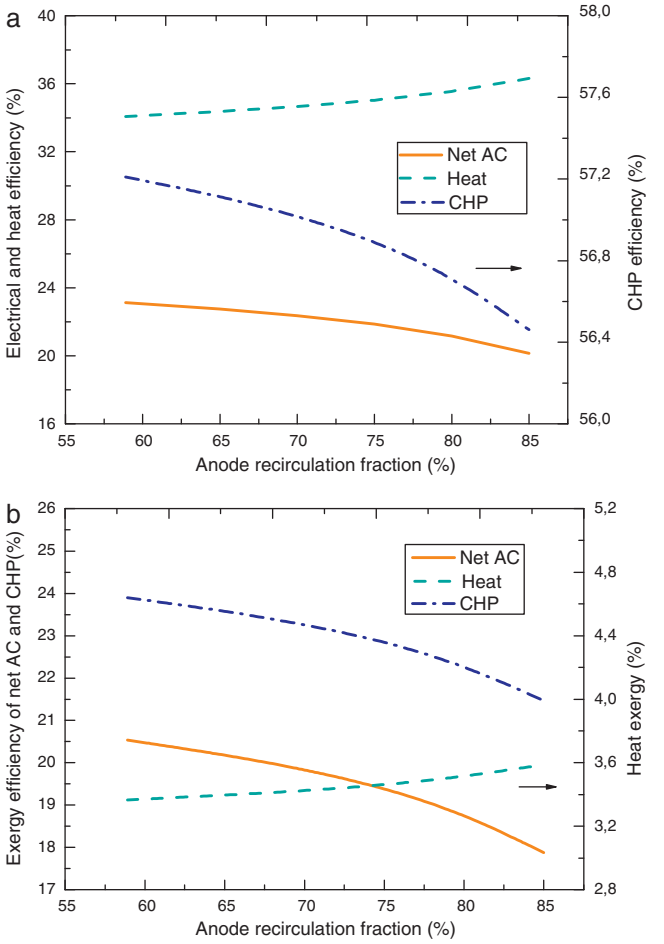

Fig. 16. (a) Influence of anode recirculation on system energy conversion efficiency and (b) influence of anode recirculation on system exergy performance.

and for preventing the carbon formation is desirable. In this work, the anode recirculation fraction is set around 62% which is in agreement with Campanari's work [25], and this value makes the oxygen to carbon ratio bigger than 2.0 which is sufficient to prevent the risk of carbon deposition in practical operations [24].

5. Conclusions and future work

A commercial SOFC CHP system (Alpha unit from Siemens-FCT) fuelled by natural gas and biosyngas from biomass gasification was evaluated by thermodynamic calculations. Two gas cleaning systems were proposed to integrate the gasifier with the SOFC CHP system.

(1) Natural gas fuelled SOFC system has a better system performance, especially with regard to electricity production, than the gasified-biosyngas fuelled SOFC systems. As of the energy conversion, the latter system offers comparable thermal efficiency although the total CHP efficiency is lower. However, the exergy efficiencies in the gasifier–SOFC systems are much lower than the natural gas fuelled SOFC system.
(2) No significant differences of the electrical efficiency were observed between SOFC systems fed by biosyngas with the two types of gas cleaning systems (cases 1 and 2). The combined high and low temperature gas cleaning system of the case 1 offers advantages when electricity production is given importance, while the high temperature gas cleaning system described in the case 2 is preferred when there is a larger heat demand. If a modification can be properly made with the SOFC CHP system for steam generation, the net AC electrical efficiency of the case 3 is increased without sacrificing too much in the total CHP efficiency.
(3) There is the possibility of carbon formation when the typical high temperature gas cleaning technologies are employed. To avoid carbon formation, steam addition seems to be a more realistic option for the system operation but it sacrifices the electrical efficiency of the system.
(4) A sensitivity study presented in this work is helpful for selecting appropriate working conditions for safe system operations and for high system efficiency.

Although anode recirculation is analyzed to simulate the functions of the ejector, there might be a difference in net AC power output for real system operations. The main reason for this difference is that the fresh fuel needs to be pressurized to a higher pressure (~3 bar) to ensure the ejector entrain a part of the anode-off gas. Apparently, this process takes more parasitic power. Hence a detailed ejector calculation is to be carried out in the near future to refine the system study presented here. These studies would be helpful for carrying out the experimental work with the system. For the experimental work, the SOFC CHP system which has been installed will be first tested using natural gas. A CTGCS which is being built is to be used to integrate the SOFC CHP system with the downdraft fixed-bed gasifier. The performance of the complete

system including the gasifier, the gas cleaning system and the SOFC CHP unit will be evaluated experimentally soon. The results from the experimental evaluations will be used to validate the modeling results presented in this work.

References

[1] C.O. Colpan, F. Hamdullahpurb, I. Dincerc, Y. Yoo, Int. J. Hydrogen Energy 35 (2009) 5001–5009.
[2] C. Athanasiou, E. Vakouftsi, F.A. Coutelieris, G. Marnellos, A. Zabaniotou, Chem. Eng. J. 149 (2009) 183–190.
[3] P.V. Aravind, T. Woudstra, N. Woudstra, H. Spliethoff, J. Power Sources 190 (2009) 461–475.
[4] A.O. Omosun, A. Bauen, N.P. Brandon, C.S. Adjiman, D. Hart, J. Power Sources 131 (2004) 96–106.
[5] J. Mermelstein, M. Millan, N. Brandon, J. Power Sources 195 (2010) 1657–1666.
[6] P.V. Aravind, J.P. Ouweltjes, N. Woudstra, G. Rietveld, Electrochem. Solid-State Lett. 11 (2008) B24–B28.
[7] J.P. Ouweltjes, P.V. Aravind, N. Woudstra, G. Rietveld, J. Fuel Cell Sci. Technol. 3 (2006) 495–498.
[8] Ph. Hofmann, K.D. Panopoulos, P.V. Aravind, M. Siedlecki, A. Schweiger, J. Karl, J.P. Ouweltjes, E. Kakaras, Int. J. Hydrogen Energy 34 (2009) 9203–9212.
[9] Ph. Hofmann, A. Schweiger, L. Fryda, K.D. Panopoulos, U. Hohenwarter, J.D. Bentzen, J.P. Ouweltjes, J. Ahrenfeldt, U. Henriksen, E. Kakaras, J. Power Sources 173 (2007) 357–366.
[10] L. Fryda, K.D. Panopoulos, E. Kakaras, Energy Convers. Manage. 49 (2008) 281–290.
[11] Ph. Hofmann, K.D. Panopoulos, L.E. Fryda, A. Schweiger, J.P. Ouweltjes, J. Karl, Int. J. Hydrogen Energy 33 (2008) 2834–2844.
[12] V. Alderucci, P.L. Antonucci, G. Maggio, N. Giordano, V. Antonucc, Int. J. Hydrogen Energy 19 (1994) 369–376.
[13] L. Fryda, K.D. Panopoulos, J. Karl, E. Kakaras, Energy 33 (2008) 292–299.
[14] R. Toonssen, N. Woudstra, A.H.M. Verkooijen, Proceedings of the 8th European Solid Oxide Fuel Cell Forum, Luzerne, Switzerland, 2008.
[15] R. Zevenhoven, P. Kilpinen, Helsinki Univ. Technol. (2001) 17–179.
[16] S.C. Bhattacharya, A.M.R. Siddique, H.L. Pham, Energy 24 (1999) 285–296.
[17] J.D. Martinez, MSc thesis (in Portuguese), Federal University of Itajuba, Brazil, 2009.
[18] P.A. Smell, J.B. son Bredenberg, Fuel 69 (1990) 1219–1225.
[19] A.V. Bridgwater, Fuel 74 (1995) 631–653.
[20] K.R. Cummer, R.C. Brown, Biomass Bioenergy 23 (2002) 113–128.
[21] Fuel Cell Technology Ltd., 5 kW SOFC Alpha Unit Operations Manual, 2005.
[22] Cycle-Tempo 5.0, TU Delft, 2006, www.cycle-tempo.nl.
[23] Phyllis, database for biomass and waste, http://www.ecn.nl/phyllis.
[24] Personal communication with Dr. Wojtek Halliop.
[25] S. Campanari, J. Power Sources 92 (2001) 26–34.
[26] S.C. Singhal, Solid State Ionics 135 (2000) 305–313.
[27] www.factsage.com.
[28] J. Mermelstein, N. Brandon, M. Millan, Energy Fuels 23 (2009) 5042–5048.
[29] G. Allen, Rural Energy Conf. (2004).
[30] H. Morita, F. Yoshiba, N. Woudstra, K. Hemmes, H. Spliethoff, J. Power Sources 138 (2004) 31–40.
[31] P. Nehter, J. Power Sources 164 (2007) 252–259.
[32] Ph. Hofmann, K.D. Panopoulosb, P.V. Aravind, M. Siedlecki, A. Schweiger, J. Karl, J.P. Ouweltjes, E. Kakaras, Int. J. Hydrogen Energy 34 (2009) 9203–9212.
[33] L.P.L.M. Rabou, R.J.C. van Leijenhorst, J.H.O. Hazewinkel, ECN-E-08-086, November, 2008.
[34] A.D. Hawkes, D.J.L. Brett, N.P. Brandon, Int. J. Hydrogen Energy 34 (2009) 9558–9569.